

## EXPERIMENTAL AND NUMERICAL ANALYSIS OF BOLTED TWO PLATES USING A DEVELOPED SHEAR THEORY

KÜRŞAT TANRIVER, MUSTAFA AY

*Institute of Pure and Applied Sciences, Marmara University, Istanbul, Turkey, and*

*Faculty of Technology, Marmara University, Istanbul, Turkey*

*corresponding author Kürşat Tanriver, e-mail: k.tanriver@hotmail.com*

In this study, a software has been developed for calculating static strength of bolted steel plates. This software has been developed by adding equations covering the bending moment that occurs during a tensile test as well as under real loading conditions. In order to test the accuracy of this program, 5 samples with the M6 bolt connection were prepared. In addition, the simulation result was compared with the experimental work performed with tensile tests and the finite element analysis made in Ansys.

*Keywords:* bolt connection, MATLAB software, experimental work, finite element analysis

### 1. Introduction

When we examine fasteners in general, we notice that there are many fastening methods, and some of them are used as main methods. Firstly rivets, then bolts, and then welded joints are used (Albiez *et al.*, 2022).

Shear stress has a significant impact on structural behaviour of bolted steel construction assemblies. There are studies using bolted plates to increase the bending capacity of beams (Yao *et al.*, 2022). Bolts are known to show significant differences in strength under combined loads (Pitrakkos *et al.*, 2021). The aim of this study is to create an algorithm that analytically calculates both the plate material and bolt strength under static loading conditions when the same type of plates are connected by bolts and to investigate its industrial applicability. Ribeiro dos Santos *et al.* (2022) presented a study on the behaviour of bolts. Zhou *et al.* (2022) investigated buckling of stainless-steel pipes due to bending and carried out a study that numerically determined them. Considering bolted parts, Rakotondrainibe *et al.* (2022) potentially optimized the shape and topology of each part as well as the position and number of the bolts. Li and Young (2021) conducted an experimental study on open section members under an eccentric load used in steel structures. Fink and Camanho (2011) investigated how composite materials affect joint stiffness of metal plywood sheets, which were made of the same material as the fastener, to increase strength in metal bolt/rivet connections. Qi *et al.* (2021) simulated experimentally materials with Abaqus software and compared the results. He *et al.* (2021) studied the high-temperature load distribution of a bolt joint structure. A two-dimensional asymmetrical model of the bolt connection structure was created and a modification of the standard metric thread profile was made according to the thread load distribution, taking into account certain properties. Giannella *et al.* (2021) carried out finite element analysis by modeling three different connections of bolts that connected various components in gasoline engines. The results were compared in terms of preprocessing time and accuracy. Li *et al.* (2020) performed calculations of dynamic stiffness of mounted beam structures and connection surfaces according to an empirical formula. They created an equivalent model of bolted connections using springs and dampers and virtual material addition methods in the Ansys software. In addition, they conducted a

modal test of the beam structure. The simulation results obtained from the theoretical modeling method were compared with modal test results. Accordingly, they demonstrated that the modeling method using spring and damping elements had higher accuracy. Guzas *et al.* (2015) created a finite element model for bolts. They conducted physical experiments involving static and dynamic stress tests. They verified the models based on test data for static and dynamic stress experiments and reported achieving a good correlation. Ibrahim (2020) worked on a finite element model of a standard bolted connection using Siemens NX software. It was observed that the modal frequencies of the three simplified models were accurately captured. Additionally, the study emphasized the effects of beam discretization and computation time. Żyliński and Buczkowski (2010) conducted an analysis of bolted connections using the finite element method. Nonlinear stiffness properties for the bolt and flange with gaskets were developed. Furthermore, they compared the finite element analysis results with experimental results. Kim *et al.* (2007) proposed four types of bolt models as finite element modeling techniques for a bolted connection. The effectiveness and usability of the bolt models were validated by comparing static experiments and modal test results. Piscan *et al.* (2010) conducted research on deformation of the contact surface of a bolted connection using finite element analysis. In that study, the maximum stress that the bolt can withstand due to the maximum stress it may be exposed to, based on the bolt preload force, was determined. Additionally, the authors noted that surface contact stiffness exhibited a nonlinear variation. Ramires *et al.* (2012) worked on a connection technique they called a semi-rigid connection design. In this study, they optimized factors such as bolt diameters and positions, spring coefficients and plate thicknesses using a genetic algorithm. They managed to increase bolt stiffness while maintaining the same material cost.

## 2. Material and method

In this article, the aim is to examine the performance of plates of the same type connected with bolted connections under static loading conditions. The goal is to develop an algorithm that analytically calculates both the plate material and bolt strength. Today, metals, alloys and composites are used in various manufacturing processes by combining them with dissolvable connection techniques. In particular, quick assembly of different manufacturing plate-type connections in steel structures is facilitated by joining them with bolted connections. From the past to the present, bolts are frequently used as fasteners in steel construction assemblies, which is a common type of structure. With the advancement of technology, there has been a growing need for development of innovative designs of such bolts (Tanriver and Ay 2020).

Tensile tests can be performed to investigate tensile performance of fasteners (Guo *et al.*, 2020). In the literature, there are numerous studies where tensile load test results of bolts are both experimentally conducted and analyzed using the finite element method (Liu *et al.*, 2021).

In addition to these, in this study, calculations were made using software with an improved equation. Furthermore, the results were compared using a triple validation method. The ultimate goal here is to measure whether widely used fasteners can withstand static forces. The accuracy of the software developed in this study was assessed by comparing the experimental results and the finite element method.

### 2.1. Material

For this article, 5 test specimens of the same type and characteristics were prepared. As a sample, two ST 37 plates with 10 mm thickness ( $h_1, h_2$ ), 100 mm width  $l_e$ , and 100 mm length  $l$  were used. The ST 37 plate has a modulus of elasticity of 210 GPa, yield strength of 235 MPa and tensile strength of 375 MPa.

A zinc-coated M6 steel bolt was used at the exact center of the plates for connection. The bolts have a length of 60 mm and were selected as hex head, 8.8 quality, and fully threaded according to the DIN 933 standard. The test specimen is shown in Fig. 1.

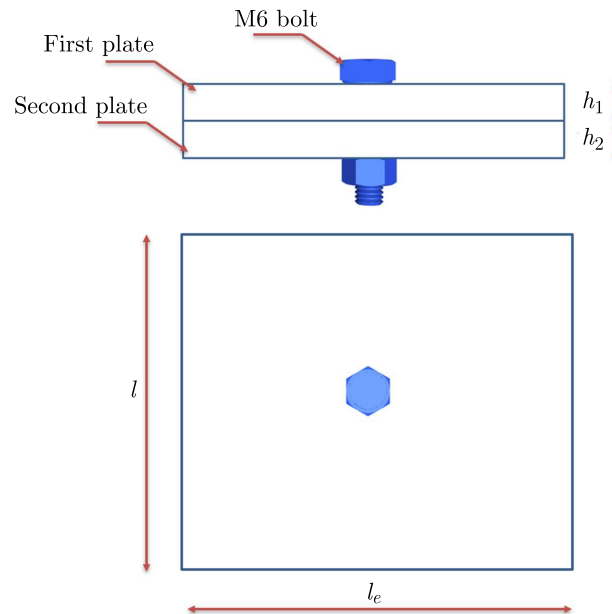


Fig. 1. Test sample

## 2.2. Method

The international standards currently used in tensile tests of metal materials include ISO 6892-1: 2016 and ASTM E8: 2016 standards. The test setup for this article was prepared in accordance with the ISO 6892-1: 2016 standard. The experiments were performed on the Instron 5569 tensile testing machine. The test specimen consists of two plates placed on top of each other and connected by a single bolt in the exact center. In this case, five specimens with the same properties were subjected to tensile load successively, with the lower jaw fixed and the upper jaw moving, forcing the bolt to be cut between the two plates. For each specimen, the tensile speed was set to 2 mm/min, and the load was gradually increased until the bolts were cut, ending the test. The first test specimen during the test and a visual of the test device are shown in Fig. 2. The test specimens were named M6-Cv1, M6-Cv2, M6-Cv3, M6-Cv-4, M6-Cv-5, respectively. The tensile test was applied to test specimens one by one in the order mentioned above.

Additionally, to investigate the static behaviour of bolted connections, analytical methods that provide stress distribution can be developed, and finite element models can be used to check their suitability. In Ansys, which is the software using these methods, numerical analysis of experimental studies on the buckling of shells and the shear load can be performed (Karasev *et al.*, 2020).

To examine the static behaviour of bolted connections, analytical methods that provide stress distribution can be developed, and finite element models can be used to verify their appropriateness (Hammami, 2022). In this article, finite element analysis was carried out using the structural Ansys R19.2 analysis module. The shear stresses were investigated afterwards.

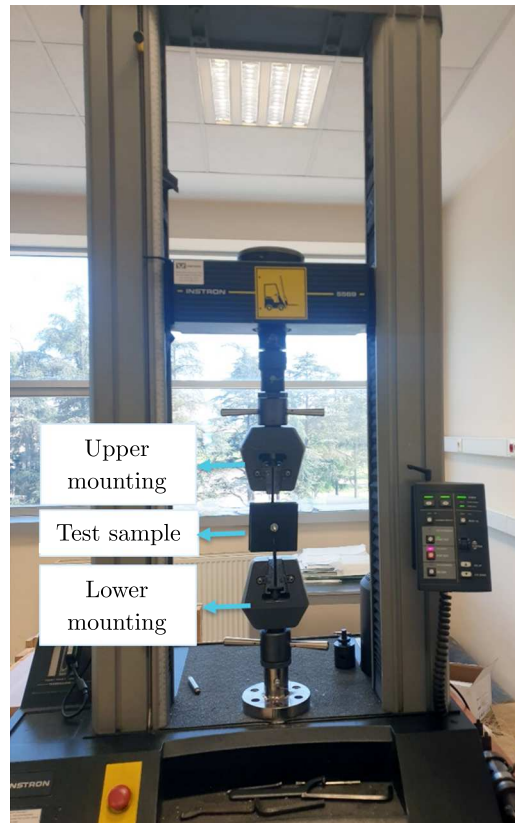


Fig. 2. Test sample

### 3. Result and discussion

#### 3.1. Experimental study and finite element analysis

Before performing the stress analysis, it is necessary to examine the loads applied to the structure. The stress-strain curves obtained from the tensile tests of the specimens are given in Fig. 3, respectively.

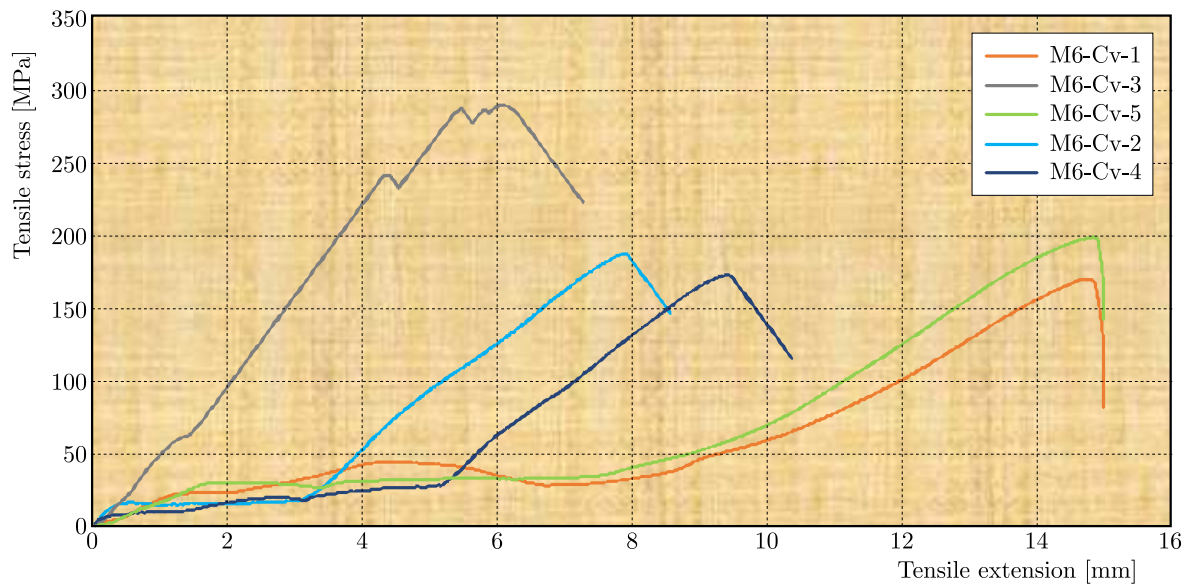


Fig. 3. Stress-extension curves

Although the test specimens were geometrically identical to each other before the tensile test, they showed differences in the test results. Some of them exhibited much more elongation resulting in fracture at lower tensile forces compared to others. In some cases, more noticeable bending occurred. A summary of the test results is given in Table 1.

**Table 1.** Tensile test results summary

Test specimen	Tensile extension [mm]	Tensile stress [MPa]	Load [N]
M6-Cv-1	14.73	170.08	10204.56
M6-Cv-2	7.85	187.69	11261.14
M6-Cv-3	12.10	289.94	17379.37
M6-Cv-4	9.37	172.81	10368.61
M6-Cv-5	14.83	198.89	11933.46
Average value		203.88 MPa	12229.42 N

Based on these results, the arithmetic mean of tensile stresses of the 5 test specimens with M6 bolt connections is found to be 203.88 MPa. Similarly, taking the average of shear forces of the bolts according to the same results, the shear force is determined to be 12229.42 N. In this study, the data obtained from the experimental results are planned to be used in both the finite element Ansys R19.2 analysis and a MATLAB code for the targeted studies. Therefore, in the “Software” Section, it is aimed to write a code based on the equations developed for this study using the MATLAB code. In Ansys R19.2 structural analysis module, simulation was performed by applying an average shear force of 12229.42 N obtained from the experimental results for the same test specimen. The analysis used a total of 235 804 finite elements and 985 717 nodes. The sweep meshing method was used, and the mesh size was set to 1 mm. The contact between the plates was defined as a surface-to-surface contact. Similarly, the connection contact between the plate-groove and the bolt threads was also defined as the surface-to-surface contact. Furthermore, for the surface-to-surface contact, tangential and normal behaviour were defined as the penalty friction and hard contact, respectively. To simulate the real constraints in the tests and to limit the displacement of one of the plates, fixed support was defined in the Y-direction. The problem was solved using the Maximum Shear Stress method. The finite element model is shown in Fig. 4.

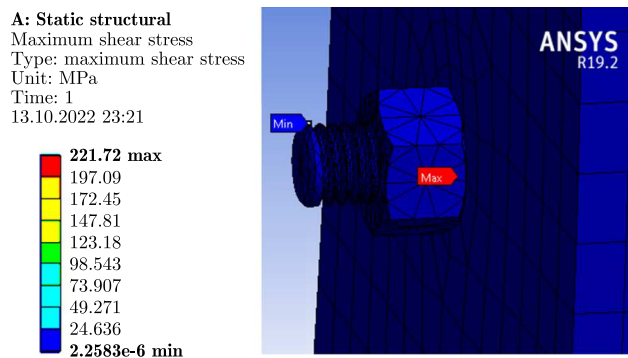


Fig. 4. Maximum shear stress analysis

Accordingly, in the finite element analysis, the maximum shear stress was found to be 221.72 MPa. The ratio between the average of the experimental results in Table 1 and the finite element result is 1.09. When we examine the studies conducted in the literature, the ratio between the experimental results and the finite element results appears to be 1.77 (Guo *et al.*, 2020), 1.08 (Rajanyam *et al.*, 2020) and 1.02 (Nguyen *et al.*, 2022). It seems that the value in this article is among the values in the current studies.

### 3.2. Modeling the plate under moment

In the literature review, it has been indicated that bolt geometry and generation of moments are improved when loads are connected eccentrically (Ansari *et al.*, 2023; Esmaeili *et al.*, 2014; Hammami, 2022; Pitrakkos *et al.*, 2021). However, no study formulating and explaining these findings through additional formulas has been found.

There are studies that claim that the load exerted on bolted connections is not actually proportional to the number of bolts and model and compare it with experimental results (Kontoleon *et al.*, 2003). Actually, it should be noted that this is because of inability to perform axial tension. The contact surface of the bolt holes providing the bolt-plate interaction should be taken into account (Ye *et al.*, 2022).

When plates are subjected to a tensile load, it is assumed that they are subjected to tensile stress in the  $y$ -axis plane as shown in Fig. 5a, and calculations are made accordingly. However, in tensile tests, it is known that this cannot be the case under real loading conditions, and the eccentricity ratio in the load test can reduce load carrying capacities (Nguyen *et al.*, 2022). Due to a non-central application of the tensile load, the plates are forced to bend, and a moment is generated.

When the stresses generated by this moment are added to simulations while calculating the shear load on the bolts, and the calculations become more accurate. The bending moment occurs at an angle in the section plane. The plate model under the moment loading is shown in Fig. 5b.

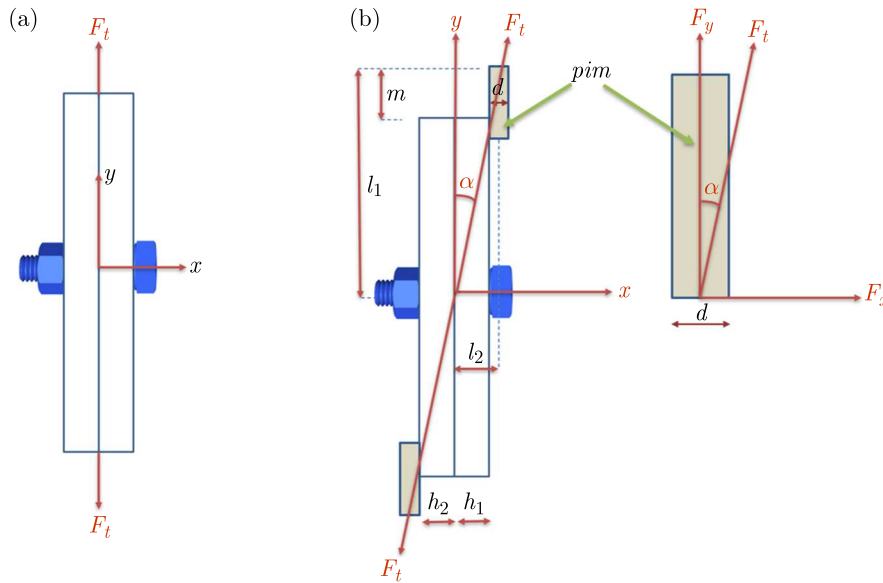


Fig. 5. The model of the plate under the moment: (a) theoretical (b) real condition

The angle  $\alpha$  that will occur in the section plane, distance  $l_1$  of the vertical force to the pivot point, distance  $l_2$  of the horizontal force to the pivot point, the vertical force  $F_y$ , the horizontal force  $F_x$  generated by these forces, and the moments  $M_1$  and  $M_2$  formed by these forces are given below

$$\begin{aligned}
 \alpha &= \tan^{-1} \frac{l_2}{l_1} & l_1 &= \frac{l}{2} + m & l_2 &= h + m & h &= h_1 = h_2 \\
 F_x &= F_T \sin \alpha & F_y &= F_T \cos \alpha & & & & \\
 M_1 &= F_x l_1 & M_2 &= F_y l_2 & & & & 
 \end{aligned}
 \tag{3.1}$$

Here,  $h$  represents plate thickness,  $l$  – length of the plate under tension,  $d$  – diameter of the bolt to which the tension jaws are connected,  $m$  effective length of tension connection, and  $F_T$  – tensile force.

The designed software consists of two stages. The first one is to determine whether the plate can withstand the forces it is subjected to, and the second one is to investigate whether the constructive strength of any bolts to be used as fastener is appropriate. In the first stage, it is necessary to calculate whether the plates can withstand the tensile force statically, and then to calculate the shear stress for bolt strength. The area affected by the tensile force  $A$ , moment of inertia  $I_z$ , stress  $\sigma$  to which the plates are exposed, the safety stress  $\sigma_{saf}$  and the plate material strength condition are given below

$$\begin{aligned}
 A &= l_e h & I_z &= l_e \frac{h^3}{12} \\
 \sigma &= \frac{F_y}{A} + \frac{M_1}{I_z} h & \sigma_{saf} &= \frac{\sigma_y}{s} & \sigma &\leq \sigma_{saf}
 \end{aligned}
 \tag{3.2}$$

Here,  $h$  represents plate thickness,  $l_e$  – plate width,  $F_y$  – force acting on the plates in the  $y$ -axis,  $I_z$  – moment of inertia,  $M_1$  – moment,  $\sigma_y$  – yield stress of the plate material, and  $s$  – safety factor.

Now, we need to examine whether the constructive strength of any of the bolts to be used as fasteners is appropriate, which is the second stage of the designed software. Due to the angled effect of the tensile force, the  $M_1$  and  $M_2$  moments were generated in the plates. Since the directions of these moments are opposite to each other, the resulting net moment  $M_{net}$ , and the tensile-compressive stress  $\sigma_{tc}$  generated by this moment are given as

$$M_{net} = M_2 - M_1 \quad \sigma_{tc} = \frac{M_{net}}{I_z} h
 \tag{3.3}$$

Here,  $h$  represents plate thickness and  $I_z$  – coefficient of the moment of inertia.

As a result of the tensile-compressive stress  $\sigma_{tc}$  generated in the plates, an additional virtual shear force will be generated that acts in the opposite direction to the bolts in the plates. The  $F_{im}$  virtual force is the maximum force that will act when the stress profile is assumed to be triangular. The intensity of the bolt within the plates changes in proportion to the area of this triangle. Therefore, the average force corresponding to the area of the triangle will be a half of the  $F_{im}$  force. The virtual force  $F_{im}$  is shown in Fig. 6.

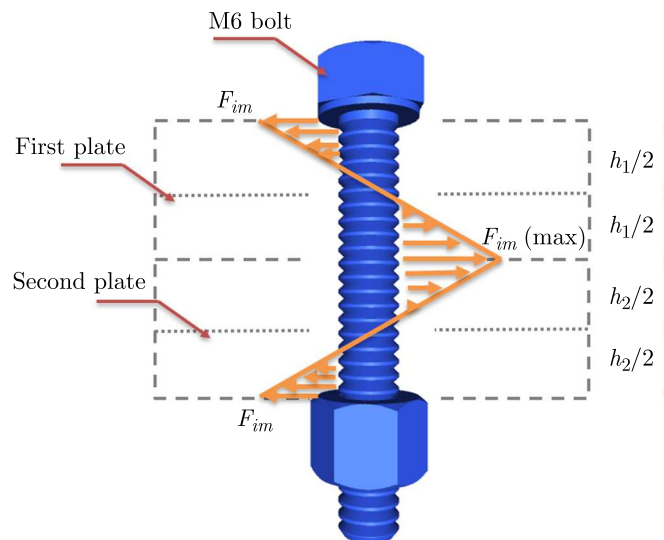


Fig. 6. Imaginary force

The crushing area  $A_{cr}$  and the virtual shear force  $F_{im}$ , with plate thickness  $h$ , are expressed by the following equations

$$F_{im} = \sigma_{tc} A_{cr} \quad A_{cr} = h D_{bolt}
 \tag{3.4}$$

Here,  $h$  represents plate thickness, and  $D_{bolt}$  – diameter of the bolt.

The total shear force per bolt  $F_{sh}$ , cross-sectional area per bolt  $A_{bolt}$ , net shear stress per bolt  $\tau_{net}$ , and the bolt shear stress strength condition are given below

$$\begin{aligned} F_{sh} &= \frac{F_y}{n} + \frac{F_{im}}{2} & A_{bolt} &= \pi \frac{D_{bolt}^2}{4} \\ \tau_{net} &= \frac{F_{sh}}{A_{bolt}} & \tau_{saf} &= \frac{\tau_s}{s} & \tau_{net} &\leq \tau_{saf} \end{aligned} \quad (3.5)$$

Here,  $n$  represents the number of bolts,  $D_{bolt}$  represents diameter of the bolt,  $F_y$  represents the force acting on the plates in the  $y$ -axis,  $F_{im}$  is the virtual force,  $\tau_s$  – shear stress of the bolt material, and  $s$  is the safety factor.

### 3.3. Software

In this Section, the equations involving bending moment have been transferred into the MATLAB code, and the code has been executed on a sample model. Additionally, to measure its accuracy, the software results have been compared with both experimental and finite element results. In the previous Section, the arithmetic average of the tensile test results for 5 samples with M6 connections, shown in Table 1, was 12229.42 N for the  $F_{real}$  load. This load was used in the Ansys maximum shear stress analysis, and the resulting stress value  $\tau_{ans}$  was 221.72 MPa.

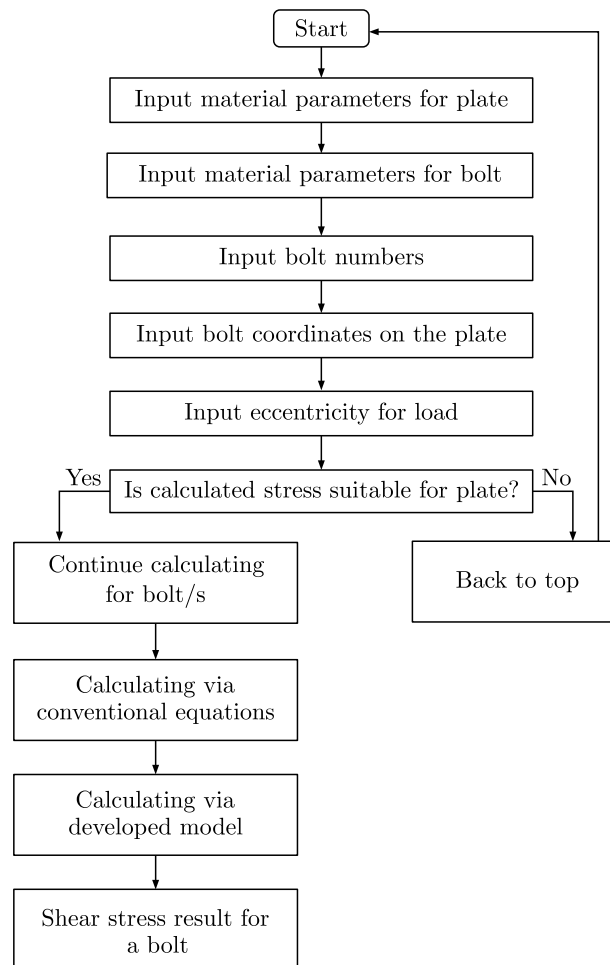


Fig. 7. Flowchart of the software procedure and result



Now, to make a proper comparison, the MATLAB program has been run on the same model dimensions shown in Fig. 1, which were used in the tensile test and finite element analysis. The load used was again the arithmetic average of the tensile test results for the 5 samples with M6 connections, shown in Table 1, with a  $F_{real}$  load of 12229.42 N. As a result, the critical stress calculated by MATLAB was 220.70 MPa. The flowchart of the software procedure and the result is shown in Fig. 7.

According to the results obtained here, the output of the MATLAB software designed for this study is 16.70 MPa higher than the average  $\tau_{real}$  (203.88 MPa) of the experimental results for the M6 bolted connection samples conducted in the laboratory environment. Additionally, it is observed that the result is 1.18 MPa lower than the output of the Ansys finite element analysis. The error rates of the MATLAB results have been determined based on both the experimental and Ansys finite element method results. The error rate relative to the laboratory test results is given as *Err test Rate*, while the error rate relative to the Ansys finite element results is given as *Err ans Rate*. The error rates are provided below

$$Err\ test\ Rate = \frac{\tau_{net} - \tau_{real}}{\tau_{real}} \tag{3.6}$$

Here, with  $\tau_{net} = 220.70$  MPa and  $\tau_{real} = 203.88$  MPa, the error rate *Err test Rate* is found to be +8.2%

$$Err\ ans\ Rate = \frac{\tau_{net} - \tau_{ans}}{\tau_{ans}} \tag{3.7}$$

Here, with  $\tau_{net} = 220.70$  MPa and  $\tau_{ans} = 221.72$  MPa, the error rate *Err ans Rate* is found to be -0.46%.

If this innovation and change was made, the simple shear stress would be given in the equation below

$$A_{bolt} = \pi \frac{D_{bolt}^2}{4} \quad \tau_{bolt-old} = \frac{F_T}{A_{bolt}} \tag{3.8}$$

Here, with the bolt diameter  $D_{bolt}$  being 6 mm, the bolt cross-sectional area  $A_{bolt}$  is found to be 28.27 mm<sup>2</sup>.

If the lowest stress value in Table 1, 10204.56 N  $F_T$  force in M6-Cv-1 sample, is considered,  $\tau_{bolt-old}$  is found to be 288.48 MPa. When considering the average value of 12229.42 N  $F_T$  force,  $\tau_{bolt-old}$  is calculated as 432.58 MPa. If the highest stress value in M6-CV-5 sample, 17379.37 N  $F_T$  force, is taken into account,  $\tau_{bolt-old}$  is found to be 614.76 MPa. Since 288.48 MPa is a closer value, the error rate is expressed below considering this value

$$Err\ test\ Rate = \frac{\tau_{net} - \tau_{real}}{\tau_{real}} \tag{3.9}$$

Here, with  $\tau_{bolt-old} = 288.48$  MPa and  $\tau_{real} = 203.88$  MPa, the error rate *Err test Rate* is found to be +41.5%.

As can be seen here, if the conventional bolt shear stress calculation was done, the current error rate would be 41.4%. However, with the modifications and calculations done by using the MATLAB program, the error rate is found to be 8.2%. The new calculation provides 33.3% more accurate results compared to the old calculation, offering designers a safer margin and benefits in terms of staying within the safety zone. In addition to all of these, a regression analysis has been performed between the values of different bolt diameters with the average force of 12229.42 N using the program. The regression analysis graph is shown in Fig. 8.

Accordingly, the determination coefficient  $R^2$  is found to be 0.9816, approaching 1. With a constant load of 12229.42 N, the equation predicts the critical stress per bolt with the independent variable of bolt diameter at a rate of 98.16%. The critical stress values written opposite the bolt diameter are taken from the MATLAB algorithm; therefore, it can be concluded that the code provides a correct stress value at a rate of 98.16%.

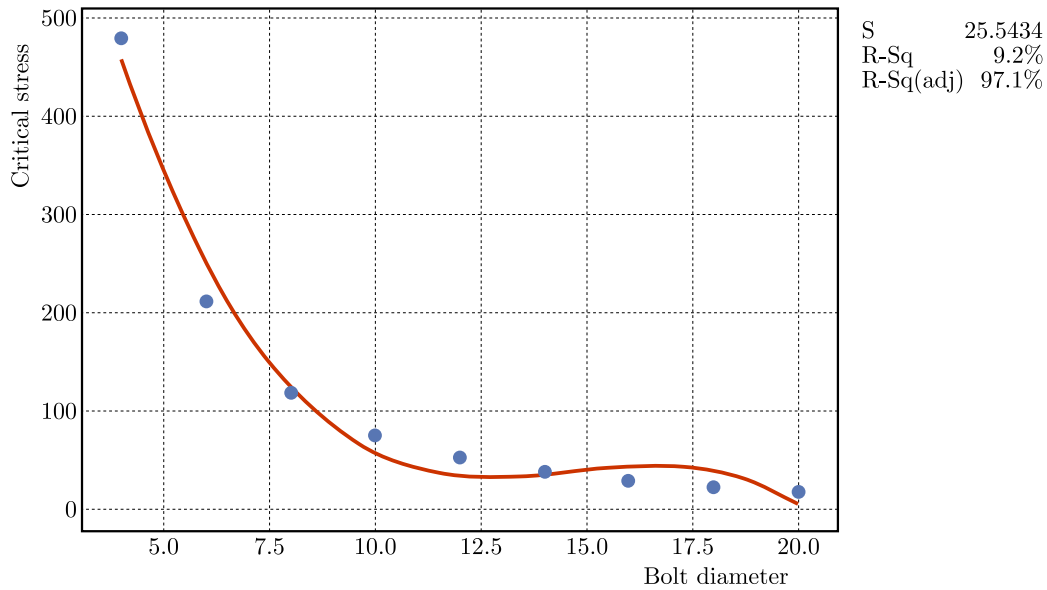


Fig. 8. Regression analysis graph

#### 4. Conclusion

In the literature review, there are studies that show the improvement of bolt geometry and the formation of moments when the loads are connected eccentrically when compared with existing models. However, no study has been found that develops and explains this by converting these quantities into equations and adding additional formulas. For that reason, codes have been added to the MATLAB software in order to calculate the moments formed by eccentricity during tension, in addition to conventional studies, and the software has been improved. The designed software consists of two stages. The first stage is to determine whether the plate used can withstand the forces it is subjected to, and the second stage is to investigate whether the constructive strength of any of the bolts used as fasteners is appropriate.

In order to investigate tensile performance of fasteners, tensile tests are performed. Generally, there are studies comparing experimental results with finite element results. There are also studies that validate numerical and experimental results for estimating the shear capacity of bolted connections. In this study, additionally, calculations are made with the help of the MATLAB software, and the results are compared in a triple validation method with both finite element and experimental method.

Although the specimens were geometrically identical to each other before tensile tests, they showed differences in the test results. In some of them, elongation was much greater compared to others, resulting in failure at lower tensile forces. In others, more visible bending occurred. According to the test results, an arithmetic average of stresses of 5 M6 connected samples with the same properties was taken, and the average stress was found to be 203.88 MPa. Also, based on the same results, the average shear load was determined to be 12229.42 N. The finite element analysis in the Ansys R19.2 structural analysis module was performed using the average shear load of 12229.42 N. Consequently, the maximum shear stress in the finite element analysis was found to be 221.72 MPa. Considering these values, the ratio between the average of the test results and the finite element analysis was 1.09. It is a value within the range of ratios between experimental and finite element results found in the literature.

Additionally, the code written with the added equations was run in MATLAB using the average shear load, which indicated a critical stress of 220.70 MPa. Based on these results, the MATLAB software developed with the improved additional formulas has error rates of +8.2%

when considering the experimental results and  $-0.46\%$  when considering Ansys finite element results.

If this innovation was not made and the conventional bolt shear stress calculation was used, the current error rate would be  $41.4\%$ . The new calculation offers a  $33.3\%$  more accurate estimate compared to the old calculation, providing designers with a safer margin and benefiting them by staying within the safety zone.

In addition to these, a regression analysis has been performed for different bolt diameters. Accordingly, the coefficient  $R^2$  was found to be close to 1,  $0.9816$  in exact. With a constant load of  $12229.42$  N, the critical stress per bolt, with the bolt diameter as an independent variable, was predicted with an accuracy of  $98.16\%$ . Since these values were obtained in MATLAB, it was also concluded that the code provided stress values with an accuracy of  $98.16\%$ .

In the future, it is aimed to develop the presented study by adding an optimization module. Thus, by preparing constraint functions for plates and bolts, the most suitable coordinates for the bolts can be determined. This will provide a more efficient and effective design process, ensuring that the connections are optimized for a specific application and requirements.

## References

1. ALBIEZ M., DAMM J., UMMENHOFER T., KAUFMANN M., VALLÉE, T., MYSLICKI S., 2022, Hybrid joining of jacket structures for offshore wind turbines – Determination of requirements and adhesive characterisation, *Engineering Structures*, **259**, 114186
2. ANSARI R., HASSANI R., GHOLAMI Y., ROUHI H., 2023, Numerical nonlinear bending analysis of FG-GPLRC plates with arbitrary shape including cutout, *Structural Engineering and Mechanics*, **85**, 2, 147-161
3. ESMAEILI F., ZEHSAZ M., CHAKHERLOU T., 2014, Investigation the effect of tightening torque on the fatigue strength of double lap simple bolted and hybrid (boltedbonded) joints using volumetric method, *Materials and Design*, **63**, 349-359
4. FINK A., CAMANHO P., 2011, Reinforcement of composite bolted joints by means of local metal hybridization, *Composite Joint and Connections*, 3-34
5. GIANNELLA V., SEPE R., CITARELLA R., ARMENTANI E., 2021, FEM modelling approaches of bolt connections for the dynamic analyses of an automotive engine, *Applied Sciences*, **11**, 10, 4343, 1-12
6. GUO X., ZONG S., GAO S., ZHU S., ZHANG Y., 2020, Ductile failure of occlusive high strength bolt connections under shear force, *Journal of Constructional Steel Research*, **168**, 105982
7. GUZAS E., BEHAN K., DAVIS J., 2015, 3D finite element modeling of single bolt connections under static and dynamic tension loading, *Shock and Vibration*, article ID 205018
8. HAMMAMI C., 2022, Numerical investigation of static behavior of bolted joints, *Journal of Theoretical and Applied Mechanics*, **60**, 3, 385-394
9. HE L., ZHANG B., GUO C., SHI W., 2021, Stress and load distribution analysis in bolt connection with modified thread profile under high temperature conditions, *Journal of Theoretical and Applied Mechanics*, **59**, 469-480
10. IBRAHIM A., 2020, *On the Effective Finite Element Simplification of Bolted Joints: Static and Modal Analyses*, Dubai: Master Thesis, Rochester Institute of Technology
11. KARASEV A., VARIANYCHKO M., BESSMERTNYI Y., KRASOVSKY V., KARASEV G., 2020, Numerical analysis of experimental research on buckling of closed shallow conical shells under external pressure, *Journal of Theoretical and Applied Mechanics*, **58**, 1, 117-126
12. KIM J., YOON J.-C., KANG B.-S., 2007, Finite element analysis and modeling of structure with bolted joints, *Applied Mathematical Modelling*, **31**, 895-911

13. KONTOLEON M., KAZIOLAS D., ZYGOMALAS M., BANIOPOULOS C., 2003, Analysis of steel bolted connections by means of a nonsmooth optimization procedure, *Computers and Structures*, **81**, 2455-2465
14. LI P., LI W., WEI P., WANG Q., 2020, Research on finite element analysis and modelling of bolted joint, *IOP Conference Series: Materials Science and Engineering*, Bristol, UK: IOP Publishing Ltd., 156-167
15. LI Q., YOUNG B., 2021, Tests of cold-formed steel built-up open section members under eccentric compressive load, *Journal of Constructional Steel Research*, **184**, 1-12
16. LIU Y., LI M., LU X., LI Q., ZHU X., 2021, Pull-out performance and optimization of a novel Interference-fit rivet for composite joints, *Composite Structures*, **269**, 114041
17. NGUYEN T.-T., THAI H.-T., LI D., WANG J., UY B., NGO T., 2022, Behaviour and design of eccentrically loaded CFST columns with high strength materials and slender sections, *Journal of Constructional Steel Research*, **188**, 1-16
18. PISCAN I., PREDINCEA N., POP N., 2010, Finite element analysis of bolted joint, *Proceedings in Manufacturing Systems*, **5**, 167-172
19. PITRAKKOS T., TIZANI W., CABRERA M., SALH N.F., 2021, Blind bolts with headed anchors under combined tension and shear, *Journal of Constructional Steel Research*, **179**, 106546
20. QI H., CHEN S., ZOU J., ZHANG H., LIU M., JU J., SANG X., 2021, Numerical study on the dynamic response of a concrete fillet steel tubular long column under axial impact by a rigid body, *Journal of Theoretical and Applied Mechanics*, **59**, 551-563
21. RAJANAYAGAM H., GUNAWARDENA T., MENDIS P., POOLOGANATHAN K., GATHEESHGAR P., DISSANAYAKE M., CORRADI M., 2022, Evaluation of inter-modular connection behaviour under lateral loads: An experimental and numerical study, *Journal of Constructional Steel Research*, **194**, 1-16
22. RAKOTONDRAINIBE L., DESAI J., ORVAL P., ALLAIRE G., 2022, Coupled topology optimization of structure and connections for bolted mechanical systems, *European Journal of Mechanics – A Solids*, **93**, 104499
23. RAMIRES F., ANDRADE S., SILVA VELLASCO P.C.G.D.S., DE LIMA L.R.O., 2012, Genetic algorithm optimization of composite and steel endplate semi-rigid joints, *Engineering Structures*, **45**, 177-191
24. RIBEIRO DOS SANTOS L., BARRETO CALDAS R., PRATES J.A., RODRIGUES F.C., CARDOSO H., 2022, Design procedure to bearing concrete failure in composite cold-formed steel columns with riveted bolt shear connectors, *Engineering Structures*, **256**, 114003
25. TANRIVER K., AY M., 2020, Topology optimization of a steel construction bolt under boundary conditions, *Euroasia Journal of Mathematics, Engineering, Natural and Medical Sciences*, **7**, 12, 31-47
26. YAO Y., HUANG H., ZHANG W., YE Y., XIN L., LIU Y., 2022, Seismic performance of steel-PEC spliced frame beam, *Journal of Constructional Steel Research*, **197**, 1-11
27. YE J., QUAN G., YUN X., GUO X., CHEN J., 2022, An improved and robust finite element model for simulation of thin-walled steel bolted connections, *Engineering Structures*, **250**, 113368
28. ZHOU F., HUANG L., LI H.-T., 2022, Cold-formed stainless steel SHS and RHS columns subjected to local-flexural interactive buckling, *Journal of Constructional Steel Research*, **188**, 106999
29. ŻYLINSKI B., BUCZKOWSKI R., 2010, Analysis of bolt joint using the finite element method, *Archive of Mechanical Engineering*, **LVII**, 3, 275-292